Published in final edited form as:
Biochemistry. 2007 August 7; 46(31): 9133–9142. doi:10.1021/bi700944j.

Direct evidence for specific interactions of the fibrinogen αC-domains with the central E region and with each other

Rustem I. Litvinov[1,*], **Sergiy Yakovlev**[2], **Galina Tsurupa**[2], **Oleg V. Gorkun**[3], **Leonid Medved**[2,*], and **John W. Weisel**[1]

1*Department of Cell & Developmental Biology, University of Pennsylvania School of Medicine, Philadelphia, Pennsylvania 19104-6058, USA*

2*Center for Vascular and Inflammatory Diseases and Department of Biochemistry and Molecular Biology, University of Maryland School of Medicine, Baltimore, Maryland 21201, USA*

3*Department of Pathology and Laboratory Medicine, University of North Carolina, Chapel Hill, North Carolina 27599-7525, USA*

Abstract

The carboxyl-terminal regions of the fibrinogen Aα chains (αC regions) form compact αC-domains tethered to the bulk of the molecule with flexible αC-connectors. It was hypothesized that in fibrinogen two αC-domains interact intramolecularly with each other and with the central E region preferentially through its N-termini of Bβ chains, and that removal of fibrinopeptides A and B upon fibrin assembly results in dissociation of the αC regions and their switch to intermolecular interactions. To test this hypothesis, we studied the interactions of the recombinant αC region (Aα221-610 fragment) and its sub-fragments, αC-connector (Aα221-391) and αC-domain (Aα392-610), between each other and with the recombinant $(Bβ1\text{-}66)_2$ and $(β15\text{-}66)_2$ fragments and NDSK corresponding to the fibrin(ogen) central E region, using laser tweezers-based force spectroscopy. TheαC-domain, but not the αC-connector, bound to NDSK, which contains fibrinopeptides A and B, and less frequently to desA-NDSK and $(Bβ1\text{-}66)_2$ containing only fibrinopeptides B; it was poorly reactive with desAB-NDSK and $(β15\text{-}66)_2$ both lacking fibrinopeptides B. The interactions of the αC-domains with each other and with the αC-connector were also observed, although they were weaker and heterogeneous in strength. These results provide the first direct evidence for the interaction between the αC-domains and the central E region through fibrinopeptides B, in agreement with the above hypothesis, and indicate that fibrinopeptides A are also involved. They also confirm the hypothesized homomeric interactions between the αC-domains and display their interaction with the αC-connectors, which may contribute to covalent cross-linking of α polymers in fibrin.

Keywords

Blood coagulation; protein interactions; fibrinogen; fibrin

Fibrinogen is a blood plasma protein involved in a number of (patho)physiological processes such as hemostasis, fibrinolysis, inflammation, angiogenesis, wound healing, and neoplasia

*To whom correspondence should be addressed: Dr. Rustem I. Litvinov, Department of Cell and Developmental Biology, University of Pennsylvania, School of Medicine, 421 Curie Blvd., 1040 BRB II/III, Philadelphia, PA 19104-6058, USA. Tel.: 215-898-9141; Fax: 215-898-9871 Email: E-mail: litvinov@mail.med.upenn.edu. Dr. Leonid Medved, Center for Vascular and Inflammatory Diseases, Department of Biochemistry and Molecular Biology, University of Maryland School of Medicine, 800 West Baltimore Street, Baltimore, MD 21201. Telephone: (410) 706-8065. Fax: (410) 706-8121. E-mail: E-mail: Lmedved@som.umaryland.edu.

(1,2). This polyfunctionality is due to the complex structure of fibrinogen molecules that have multiple binding sites, either constitutively open or exposed after precise enzymatic cleavage and/or conformational rearrangement. The ability to polymerize upon the action of thrombin is the unique property of fibrinogen that mainly determines its physiological significance.

Structurally, fibrinogen is a 45 nm-long elongated dimer composed of three pairs of non-identical polypeptide chains, designated Aα, Bβ, and γ (Fig. 1). The N-termini of the six chains, cross-linked by a cluster of disulfide bonds, form a central part, hence named "N-terminal disulfide knot" (3). The C-termini of Bβ and γ chains form globular modules on each end of the molecule separated from the central part by triple-helical coiled-coils (4,5). The C-terminal portions of the Aα chains extend from the coiled-coils and form αC regions, each comprising about two thirds of the Aα chain (residues 221–610 in human fibrinogen). The αC region was shown to consist of a relatively compact C-terminal portion named αC-domain (residues 392–610) attached to the bulk of the molecule via a flexible tether named αC-connector (residues 221–391) (6–8).

Functionally, αC regions of fibrinogen are implicated with a number of important molecular interactions including those in fibrin assembly, which are yet not well understood. Fibrin assembly starts when thrombin converts fibrinogen into fibrin monomer by cleaving a short N-terminal portion of the Aα chains called fibrinopeptide A (FpA). Then, the newly formed desA-fibrin monomers spontaneously self-assemble into two-stranded oligomeric protofibrils. Once the protofibrils reach a critical length, they aggregate laterally to form fibers, which are organized into the branched network, a fibrin clot. After fibrin has partially formed, thrombin cleaves fibrinopeptides B (FpB) from the N-terminal portions of the Bβ chains (9,10); this reaction gives rise to additional intermolecular interactions that reinforce the clot (11,12). Finally, the mature clot is stabilized by covalent cross-linking of specific amino acids by a transglutaminase, factor XIIIa (1,2,13,14). The notion that αC regions are involved in fibrin formation is based on three clusters of data: (i) clot formation is slowed and the clot structure is perturbed when αC regions are removed from fibrinogen either proteolytically (15–19) or as a result of a natural/artificial genetic defect (20–32); (ii) isolated αC fragments (19,33,34) or αC-specific antibodies (35,36) interfere with clot formation; (iii) αC regions polymerize and can be cross-linked by factor XIIIa, thus contributing to the clot stability (33,37–40).

It has been hypothesized that in fibrinogen the αC-domains interact intramolecularly with each other and with the central E region via FpB, while during fibrin assembly, they dissociate following the FpB cleavage and switch from intra- to intermolecular interaction (6,17,19,33, 41). Although this "intra- to intermolecular switch" hypothesis coherently accounts for the location of the αC-domains in fibrinogen and fibrin and suggests a possible mechanism for the exposure of their multiple binding sites upon conversion of fibrinogen into fibrin, it is not universally accepted (42). The major reason for the lack of consensus is that this hypothesis is based mainly on low resolution data obtained by electron microscopy. In order to test this hypothesis, we used laser tweezers-based force spectroscopy to examine binding specificity and measure the binding strength of fibrin(ogen) fragments, representing the full-length αC region or its constituents, αC-domain and αC-connector, as well as the fragments, bearing N-terminal portions of Bβ chains (BβN-domains) (Fig. 1). The laser tweezers technique that enables quantification of individual protein-protein interactions is based on the ability of the optical system to measure the rupture forces of two surface-bound protein molecules (43–45). Recently, we used this technique to examine the role of various molecular interactions, other than those mediated by αC-domain, in fibrin polymerization (41,46,47). Here we provide direct evidence for specific binding of the isolated αC-domain to the FpB-containing fibrinogen BβN-domains, but not to the fibrin βN-domains lacking FpB. In addition, we show that the αC-domains interact with each other, but their association is weaker than the αC-BβN binding.

MATERIALS AND METHODS

Recombinant fibrin(ogen) αC-fragments

The recombinant αC-fragment corresponding to the human fibrinogen αC-region (residues Aα221-610) and its constituents, αC-connector (residues Aα221-391) and αC-domain (residues Aα392-610), were produced in *E. coli*, purified and refolded as described earlier (7, 48). The purity of all fragments was confirmed by SDS-PAGE; the fragments were concentrated to 1.0–2.0 mg/ml and kept at 4°C.

Recombinant fibrin(ogen) (B)βN-containing fragments and the monoclonal antibody

The recombinant $(Bβ1\text{-}66)_2$ fragment mimicking the dimeric arrangement of the Bβ chains in fibrinogen, which form two BβN-domains (Fig. 1G), was produced in *E. coli* and purified as described elsewhere (49). To produce the activated $(β15\text{-}66)_2$ fragment, corresponding to fibrin βN-domains lacking FpB (Fig. 1H), $(Bβ1\text{-}66)_2$ was treated with thrombin and then purified as described earlier (49). The purity of non-activated and activated (B)βN-containing fragments was confirmed by SDS-PAGE. The anti-Bβ1-21 18C6 monoclonal antibody (50,51) was purchased from Accurate Chemicals (Westbury, NY).

NDSK fibrin(ogen) fragments

NDSK fragment, obtained by digestion of fibrin(ogen) with CNBr, is composed of two of each chain Aα1-51, Bβ1-118, and γ1-78 linked together by 11 disulfide bonds (52,53). Using the procedure described elsewhere (46,52), we prepared three variants of NDSK fragments: NDSK retaining both FpA and FpB (Fig. 1D) by CNBr cleavage of human plasma fibrinogen; desA-NDSK lacking FpA (Fig. 1E) by CNBr cleavage of fibrin clotted with batroxobin; and desAB-NDSK lacking both FpA and FpB (Fig. 1F) by CNBr cleavage of fibrin clotted with thrombin. Purified NDSK fragments were characterized by SDS-PAGE, dialyzed against 20 mM HEPES buffer, pH 7.4, containing 150 mM NaCl, and stored at −80 °C.

Coating surfaces with proteins

Surfaces coated with the interacting proteins were prepared basically as described previously (41,44,46). One of the interacting proteins was bound covalently to 5 μm spherical silica pedestals anchored to the bottom of a chamber. Pedestals coated with a thin layer of polyacrylamide were activated with 10% glutaraldehyde (1 hr, 37°C), washed thoroughly with 0.055M borate buffer pH 8.5, after which 1 mg/ml of a protein in 20 mM HEPES, pH 7.4 with 150 mM NaCl was inserted into the chamber and allowed to immobilize for 2 hrs at 4°C. After washing the chamber with 20 volumes of the same buffer to remove the unbound protein, 2 mg/ml bovine serum albumin (BSA) in 0.055 M borate buffer, pH 8.5, with 150 mM NaCl was added as a blocker (1 hr, 4°C). In control experiments, the BSA-containing buffer was added right after glutaraldehyde activation followed by washing of the chamber. To convert BβN-domains to βN-domains on the surface, the immobilized BβN-domain-containing fragments were treated with human thrombin (1 U/ml, 37°C, 1 hr), followed by washing of the chambers with 20 volumes of cold (4°C) 100 mM HEPES pH 7.4 containing 150 mM NaCl, 3 mM $CaCl_2$, 2 mg/ml BSA, and 0.1% (v/v) Triton X-100 about 30 min before the measurements. All the procedures were performed at 0–4°C and the chambers containing protein-coated surfaces were stored at 4°C and used within 3 hrs.

The other interacting protein was bound covalently to carboxylate-modified 1.87 μm latex beads using N-(3-dimethylaminopropyl)-N'-ethylcarbodiimide hydrochloride (Sigma, St. Louis, MO) as a cross-linking agent (46). 2 mg/ml BSA in 0.055 M borate buffer, pH 8.5, was used as a blocker. The protein-coated beads were freshly prepared, stored on ice and used within 3 hrs. The surface density of all the proteins was at the point of surface saturation, since

further increase of the time of immobilization did not augment the maximal binding probability; nonetheless, the fraction of reactive molecules that have a conformation and orientation compatible with binding was indeterminate.

The model system to study protein-protein interactions

We used a laser tweezers-based model system to study interactions between two surface-bound proteins (44–46). Laser tweezers are an optical system that use laser light to trap and manipulate dielectric particles such as small latex beads (43,54,55). External forces applied to the trapped particle can be accurately measured because the angular deflection of the laser beam is directly proportional to the lateral force applied to the particle (56–58).This system permits the measurement of discrete rupture forces produced by surface-bound molecular pairs during repeated intermittent contact (44,45).

To study particular protein pairs, fibrin(ogen) fragments of interest were bound to pedestals and beads. In most cases, the αC region fragment and NDSK fragments were covalently bound to stationary pedestals anchored to the inner surface of a flow chamber, while the smaller proteins [αC-domain, αC-connector, $(B\beta 1\text{-}66)_2$ and $(\beta 15\text{-}66)_2$] were bound to the moving latex beads. In a number of experiments, the interacting proteins were immobilized on the opposite surfaces, which did not cause a difference in results. The suspension of protein-coated beads (10^7/ml) in 100 mM HEPES buffer, pH 7.4, containing 150 mM NaCl, 3 mM $CaCl_2$, 2 mg/ml BSA, and 0.1% (v/v) Triton X-100 was then flowed into the chamber. One of the latex beads was trapped by a focused laser beam and moved in an oscillatory manner so that the bead was intermittently in contact with a stationary pedestal. The tension produced when a protein on the latex bead interacted with a complementary molecule(s) on the anchored pedestal was sensed and displayed as a force signal that was proportional to the strength of protein-protein binding(46). Rupture forces from many interactions were collected and displayed as normalized force spectra histograms for each experimental condition. The binding experiments were performed at room temperature in 100 mM HEPES buffer, pH 7.4, containing 150 mM NaCl, 3 mM $CaCl_2$ with 2 mg/ml BSA and 0.1% (v/v) Triton X-100 added to reduce non-specific interactions.

Measurement of binding strength, data processing, and data analysis

The position of the optical trap and hence a protein-coated latex bead was oscillated in a triangular waveform at 1 Hz with a pulling velocity of 1.8 μm/s, which corresponded to a loading rate of 800 pN/s. Contact duration between interacting surfaces varied from 10 to 100 ms. Rupture forces were collected at 2000 scans per second (0.5 ms time resolution). The results of many experiments under similar conditions were averaged so that each rupture force histogram represented from 10^3 to 10^4 repeated contacts of more than 10 different bead-pedestal pairs. Individual forces measured during each contact-detachment cycle were collected into 10 pN- or 5 pN-wide bins. The number of events in each bin was plotted against the average force for that bin after normalizing for the total number of interaction cycles. The percentage of events in a particular force range (bin) represents the probability of rupture events at that tension. Optical artifacts observed with or without trapped latex beads produce signals that appeared as forces below 10 pN. Accordingly, rupture forces in this range were not considered when the data were analyzed. The rupture force histograms were fit empirically with multimodal Gaussian curves using Origin 7.5® (OriginLab Corp., Northampton, MA) to determine the position of a peak that corresponds to the most probable rupture force.

RESULTS

Interactions of the αC region and its constituents with the (B) βN-domains

To check directly whether the N-terminal portions of the fibrinogen Bβ chains bind to the C-terminal portions of the Aα chains, the recombinant $(B\beta 1\text{-}66)_2$ fragment containing two disulphide-linked BβN-domains* (Fig. 1G) was exposed to the αC region fragment* and its sub-fragments, comprising the αC-domain and αC-connector (Fig. 1A–C). [*For the sake of simplicity, the word "fragment" is often omitted hereinafter and the dimeric (B)βN-domain-containing fragments, $(B\beta 1\text{-}66)_2$ and $(\beta 15\text{-}66)_2$, are called (B)βN-domains.] For the interactions of the αC region and αC-domain with the BβN-domains, similar multimode rupture force spectra in the range of 10 to 170 pN were detected with three peaks at 30–35 pN, 70–80 pN, and 115–125 pN that were fitted with the Gaussians (Fig. 2A and 2B). The peaks had decreasing probability of interaction with larger forces, and the cumulative probability of all meaningful rupture forces >10 pN was as much as 82% for the αC region and 83% for the αC-domain (Table 1). By contrast, the αC-connector was significantly less reactive with the BβN-domains, with no characteristic peaks and the cumulative probability of forces >10 pN equal to only 49% ($p<0.01$) (Fig. 2C, Table 1).

When we replaced the fibrinogen BβN-domains with the fibrin βN-domains (Fig. 1H), the interactions of the αC region and αC-domain largely vanished and the cumulative binding probability dropped about 2-fold ($p<0.01$) (Fig. 2D and 2E; Table 1), while the interactions of the αC-connector remained unchanged (Fig. 2F). The bar graph in Fig. 2I clearly shows that removal of FpB from the BβN-domains significantly reduced the binding probability of the αC region and αC-domain, suggesting that the interactions were mediated by FpB. At the same time, reactivity of the αC-connector did not seem to depend on the presence of uncleaved FpB, indicating that the binding in the latter case was non-specific, i.e., not mediated specifically by the N-terminal portions of the Bβ chains.

To verify the effect of FpB removal on the interactions of the αC region and αC-domain, we treated the surface-bound BβN-domains with thrombin (1 U/ml, 37°C, 1 hr), which resulted in FpB cleavage and formation of the fibrin βN-domain right on the surface. The rupture force spectrum of the interactions of the thrombin-treated BβN-domains and the αC region (Fig. 2G) appeared as a broad range of forces without well-defined peaks observed in Fig. 2A and resulted in significant reduction of binding probability (from 82% to 52%, $p<0.01$). The mAb against the N-terminal 1–21 portion of the Bβ chain caused an even more profound inhibitory effect on the αC-BβN interactions with a binding probability of 29% (Fig. 2H, Table 1), further confirming that the interactions with the αC-domain were mediated by the N-terminal portions of the Bβ chains. When the surface density of the BβN-domain or the αC-domain was reduced 10-fold, the cumulative binding probability dropped to 35% and 26%, respectively (Table 1), thus providing additional evidence for the specificity of interactions between the αC- and BβN-domains.

Interactions of the αC region and αC-domain with NDSK

To check whether or not the binding mediated by the N-terminal portion of the Bβ chain was limited to the specific properties of the $(B\beta 1\text{-}66)_2$ fragment, we repeated the binding experiment with different forms of N-terminal disulphide knot (NDSK), comprising the central part of fibrin(ogen) (Fig. 1D–F). Binding of the αC region fragment and its active sub-fragment, αC-domain, was examined for three types of the NDSK fragments that differed by their fibrinopeptide composition. Both FpA and FpB were intact in the NDSK (Fig. 1D), while only FpA was missing in desA-NDSK (Fig. 1E), and both FpA and FpB were missing in desAB-NDSK (Fig. 1F). For the interactions of the NDSK fragment with the αC region, a relatively sharp and prominent peak was observed with the most probable rupture forces at 44±13 pN

and higher forces of decreasing probability up to 150 pN. The overall reactivity of the proteins was high, and the cumulative binding probability reached 88% (Fig. 3A, Table 1). The interactions of the αC region with desA-NDSK (Fig. 3B) were much less pronounced compared to the NDSK (Fig. 3A) with the cumulative binding probability of only 59% ($p<0.01$), indicating that the N-terminal portions of the Aα chains are also involved in the binding with the αC region. Despite the reduction of the overall binding probability, a minor peak remained at 41±22 pN (Fig. 3B, dashed line), similar to the one resulting from the interactions of the αC region with NDSK (Fig. 3A, dashed line). The removal of FpB in addition to FpA caused almost complete abrogation of the interactions of desAB-NDSK with the αC region (Fig. 3C). The range of rupture forces significantly diminished to 10–90 pN and the cumulative probability for these interactions dropped to 15%, the value similar to the non-specific background interactions between the αC region and BSA (Table 1).

In accordance with the behavior of the αC region, the αC-domain also interacted with the NDSK readily, producing a wide range of forces from 10 pN to 170 pN, which could be very roughly segregated into two peaks centering at 52±17 and 128±26 pN (Fig. 3D, dashed line). As it was shown for the αC region, the αC-domain was reactive with desA-NDSK (Fig. 3E), however, the cumulative probability was somewhat lower than with the NDSK (71% vs. 89%, $p<0.05$). The moderate peak centering at 34±17 pN could be revealed after fitting analysis suggesting that the cleavage of FpA only partially reduced the interactions of NDSK with the αC-domain. Accordingly, the mAb against Bβ1-21 did not completely abrogate the interactions between the αC domain and NDSK with the cumulative probability remaining at the level of 56% (Table 1), far above those of the non-specific background, indicating that the blocked N-terminal portions of the Bβ chains comprise only a part of the interaction site(s) for the αC domain. By contrast, the inhibition of binding between the αC-domain and desA-NDSK with the anti-Bβ1-21 mAb was almost complete (Fig. 3F), confirming the important contribution of the N-terminal portions of the Bβ chains to the reactivity of NDSK with the αC-domain. The removal of FpB from desA-NDSK caused abrogation of the interactions of desAB-NDSK with the αC-domain (Table 1), as it did with the αC region. Comparing the histograms depicted in Fig. 3 and the data shown in Table 1, it is clear that the presence of both FpA and FpB was important for the interaction of the NDSK fragments with the αC region and αC-domain.

Interactions of the αC region, αC-domain, and αC-connector with each other

To check directly whether the αC region and its constituents, the αC-domain and αC-connector, can bind to each other, they were allowed to interact in different combinations. The pedestal-bound αC region reacted with the αC region coupled to a bead (Fig. 4A); similarly, the pedestal-bound αC-domain reacted with the αC-domain coupled to a bead (Fig. 4B). Both types of interactions produced similar rupture force spectra ranging from 10 pN to 65 pN with three peaks centering at about 20 pN, 40 pN, and 50 pN. The cumulative probabilities of those interactions were very similar, 62% and 63% for the αC-domain and αC-connector, respectively (Table 1). The probabilities were, however, significantly smaller ($p<0.05$) than those observed for the interactions of the αC region and αC-domain with the BβN-domains and NDSK, despite comparable surface densities of the reacting proteins. The αC region and αC-domain both were poorly reactive with the αC-connector as inferred from the relatively low binding probabilities (26% and 31%, respectively); however, they formed moderate peaks of rupture forces at about 25–30 pN, indicating that the proteins were not fully inert (Fig. 4C and D; Table 1). When the αC-connector was exposed to itself, the interactions formed a decreasing spectrum of rupture forces without any peaks and with a binding probability of 27% (Fig. 4E), characteristic of the non-specific protein-protein interactions.

DISCUSSION

The long-standing interest in the role of the C-terminal parts of the fibrinogen Aα chains, referred to as "αC-domains", in fibrin polymerization (6,8,15–19,22,26,33,35,36,38–40,59–61) has led to the current notion that the αC-domains are important participants of fibrin clot formation, although this is still controversial (42). There is evidence that the αC-domains accelerate fibrin polymerization and make the ultimate clot structure more stable, stiff, and resistant to fibrinolysis (32). It has been proposed that in fibrinogen the αC-domains interact intramolecularly with each other and with the central region and, during fibrin assembly, the αC-domains switch from intra- to intermolecular interaction, thus promoting lateral aggregation of protofibrils (6,17). This hypothesis is based largely on the indirect evidence obtained by differential scanning calorimetry (59,60) and transmission electron microscopy (19,33,61–63), demonstrating that in fibrinogen a pair of the αC-domains shows up as a globular particle near the central region, while in fibrin monomer they extend away from the backbone, forming two separate appendages. Many other experiments that utilized heterogeneous fibrin(ogen) degradation products or heterozygous dysfibrinogens (6) get at the αC-mediated interactions far less directly, making interpretation difficult and sometimes ambiguous. Therefore, the ability of the αC domains to form specific associations still has been a matter of debate (42). In this study, for the first time, we directly observed and quantified the bimolecular interactions between recombinant fibrin(ogen) fragments containing the C-terminal parts of the Aα chains and the N-terminal portions of the Bβ chains, thus reproducing the intramolecular associations of the αC-domains with the central part of the fibrinogen molecule and between each other. The results clearly show that there are specific interactions between the αC-domains and the central E region, which are partially reduced after cleavage of FpA and are fully abrogated upon FpB removal. In addition, the αC-domains form relatively weak homomeric associations, which are still stronger and more stable than the non-specific background protein-protein interactions.

Although the whole αC region (Aα221-610) is reactive with the fragments derived from the fibrinogen E region, its binding capacity is largely determined by the relatively compact C-terminal portion, the αC-domain (Aα392-610), but not by the unstructured N-terminal αC-connector (Aα221-391). The αC region and αC-domain fragments both had remarkable and similar rupture force profiles with $(B\beta 1\text{-}66)_2$ (Fig. 2A and B) and NDSK (Fig. 3A–B and D–E), while the αC-connector was significantly less reactive and displayed a qualitatively different behavior, showing rupture force profiles of lower cumulative probability (Table 1) without well-defined force peaks (Fig. 2C and F). The overall force profile with exponentially decreasing binding probability with larger forces, observed for the αC connector, is characteristic of non-specific background interactions (45, 64). In addition, the reactivity of the αC-connector, unlike the αC region and αC-domain, was independent of the presence or absence of FpB in the BβN- or βN-domains (Fig. 2C, F and I), indicating that the binding was not mediated specifically by the N-terminal portions of the Bβ chains and rather reflected non-specific protein-protein interactions. Therefore, it is the αC-domain, but not the αC-connector that serves as the reactive part of the αC region and is directly involved in the molecular interactions with the BβN-domains.

It was hypothesized that intramolecular interactions between the αC-domains and the central E region of fibrinogen were mediated by the N-terminal portions of the Bβ chains, including FpB (19). This assumption was tested and proved in this paper by direct exposure of the αC regions and αC-domains to the recombinant $(B\beta 1\text{-}66)_2$ fragment mimicking the dimeric arrangement of the BβN-domains in fibrinogen. Both the αC regions and αC-domains readily reacted with $(B\beta 1\text{-}66)_2$ producing a multimode rupture force spectrum (Fig. 2A and B). These interactions vanished when this BβN-domain-containing fragment was replaced with the $(\beta 15\text{-}66)_2$ fragment, containing two βN-domains (Fig. 2D, E and I; Table 1). In addition, the

interactions of the αC regions and αC-domains with $(B\beta 1\text{-}66)_2$ could be abrogated by direct cleavage of FpB by thrombin on the surface (Fig. 2G) or blocking the N-terminal portions of the Bβ chains by the anti-Bβ1-21 mAb (Fig. 2H). The susceptibility of the interactions to the presence or absence of exposed FpB indicates that the binding is specifically mediated by the N-terminal 1–14 portions of the Bβ chains corresponding to FpB.

When $(B\beta 1\text{-}66)_2$ and $(\beta 15\text{-}66)_2$ were replaced with the NDSK fragments, which represent larger and more complex parts of fibrin(ogen) central E region, the critical importance of FpB for binding with the αC-domains has been generally confirmed. In addition, it was found that the cleavage of FpA from NDSK, resulting in formation of desA-NDSK, partially reduced the ability of the αC regions and αC-domains to bind the isolated central E region (Fig. 3A–B and D–E). Further cleavage of FpB from desA-NDSK, resulting in formation of desAB-NDSK, precluded binding to the αC regions (Fig. 3C), as did the treatment of desA-NDSK with the anti-Bβ1-21 mAb (Fig. 3F). These findings indicate that, in addition to FpB, the N-terminal portions of the Aα chains are also involved in the intramolecular interactions between the αC-domains and the central E region of fibrinogen. It should be noted that the cleavage of FpA itself does not seem to be sufficient for dissociation of the αC-domains from the central E region, as revealed by the previous electron microscopy analysis of desA- and desAB-fibrin (33). Thus, the FpB-mediated interactions appear to be critical for formation and maintaining of the intramolecular complex between the αC-domains and the central E domain in fibrinogen, while the FpA-αC interactions are likely to reinforce this complex and contribute to its stability.

Detailed analysis of the rupture force spectra enables us to quantify the strength of interactions at the single-molecule level. There are several indirect arguments favoring the idea that the three decreasing peaks of rupture force histograms in Fig. 2A and B are indicative of the single, double, and triple αC-BβN binding, respectively. First, the maximum values of the weak (20–40 pN), intermediate (50–90 pN), and strong (100–150 pN) force peaks are roughly quantized, as would be predicted if they represent multiples of the bimolecular interactions (65). Second, the observed decreasing peak areas generally correspond to statistically predicted relative probabilities of the single, double, and triple molecular interactions. Third, the stronger forces are more susceptible to the inhibitory effects of FpB cleavage and the mAb treatment (Fig. 2 and Fig. 3), which is consistent with the assumption that the stronger forces reflect multiple interactions and, therefore, disappear first. Fourth, the high incidence of multiple intermolecular interactions is confirmed by the relatively common occurrence of stepwise detachment of the interacting surfaces (10–20%). Taken together, these considerations suggest that the binding strength of the individual αC-BβN interactions represented by the weakest peaks in the force spectra should be about 20–40 pN.

The hypothesized ability of the αC-domains to switch from intra- to intermolecular interaction during fibrin assembly implies that they bind each other specifically. This possibility was proved earlier by the fact that αC regions form homopolymers mimicking the arrangement of the αC-domains in fibrin (33,39), although the bimolecular binding between the isolated αC regions and/or its constituent parts has never been demonstrated. Our data clearly show that the αC regions do interact with each other at the single-molecule level and that the binding is mostly mediated by the αC-domains rather than the αC-connectors (Fig. 4,Table 1). The rupture force histograms produced by the αC-αC interactions differ from the αC-BβN binding in two respects; first they are significantly weaker (<60 pN vs. <160 pN, respectively) and, second, they seem to be more heterogeneous since the areas of the first, second, and third peaks are not very different (Fig. 4A). Although it is tempting to attribute the weakest peak in the force spectrum to single-molecule binding, with other peaks being multiples, the remarkable heterogeneity of the interactions does not allow doing that unambiguously. The complexity of these peaks may reflect multiple binding sites involved in αC-αC interactions. Indeed, at least two different types of binding sites are necessary to yield the linear α-polymers formed by the

αC-domains (6). Therefore, we infer that the αC-domains can form relatively weak and unstable homomeric associations. In fibrinogen, these associations are reinforced by the interactions of the αC-domains with the central E region via FpA and FpB. In fibrin, the αC-αC interactions are reinforced by the covalent factor XIIIa-mediated cross-linking.

It is noteworthy that the interactions revealed in this study between the fragments corresponding to the αC-domain and αC-connector, although quite weak and infrequent (Fig. 4D), still exceed the nonspecific background (Fig. 4F). This suggests that they have a specific component and may reflect those occurring in fibrin. To speculate about a possible physiological role of these interactions, one should recollect that the reactive Lys and Gln residues involved in covalent cross-linking of αC regions are located exclusively in their αC-domains and αC-connectors, respectively (38). This implies that in order to form cross-linked α polymers in fibrin, factor XIIIa should cross-link the αC-domains and αC-connectors of the neighboring molecules. In this case, the non-covalent interactions between the αC-domains and αC-connectors may bring them together and provide proper orientation of the cross-linking sites to facilitate the covalent cross-linking and thereby reinforcement of α polymers in fibrin.

In conclusion, these results confirm the existence of the intramolecular interactions in fibrinogen between the αC-domains and the central E region. They provide the first direct evidence that these interactions are mediated by fibrinopeptides B and that fibrinopeptides A are also involved. In addition, the specific interactions were demonstrated between two identical αC-domains and between the αC-domains and the αC-connectors. Taken together, these results support the “intra- to intermolecular switch” hypothesis and provide insight into various αC-mediated interactions in fibrinogen and fibrin.

Acknowledgements

This work was supported by grants HL-30954 (to J.W.W.) and HL-56051 (to L.M.) from the National Institutes of Health.

LIST OF ABBREVIATIONS

FpA, fibrinopeptide(s) A; FpB, fibrinopeptide(s) B; NDSK, N-terminal DiSulphide Knot; desA-NDSK, N-terminal disulphide knot with cleaved fibrinopeptides A; desAB-NDSK, N-terminal disulphide knot with cleaved fibrinopeptides A and B; SDS-PAGE, sodium dodecyl sulfate polyacrylamide gel electrophoresis; HEPES, 4-(2-hydroxyethyl)-1-piperazineethanesulfonic acid; BSA, bovine serum albumin; mAb, monoclonal antibody.

REFERENCES

1. Weisel JW. Fibrinogen and fibrin. Adv. Protein Chem 2005;70:247–299. [PubMed: 15837518]
2. Mosesson MW. Fibrinogen and fibrin structure and functions. J Thromb Haemost 2005;3:1894–1904. [PubMed: 16102057]
3. Blomback B, Blomback M, Henschen A, Hessel B, Iwanaga S, Woods KR. N-terminal disulphide knot of human fibrinogen. Nature 1968;218:130–134. [PubMed: 4296305]
4. Brown JH, Volkmann N, Jun G, Henschen-Edman AH, Cohen C. The crystal structure of modified bovine fibrinogen. Proc Natl Acad Sci U S A 2000;97:85–90. [PubMed: 10618375]
5. Yang Z, Kollman JM, Pandi L, Doolittle RF. Crystal structure of native chicken fibrinogen at 2.7 A resolution. Biochemistry 2001;40:12515–12523. [PubMed: 11601975]
6. Weisel JW, Medved L. The structure and function of the αC domains of fibrinogen. Ann N Y Acad Sci 2001;936:312–327. [PubMed: 11460487]
7. Tsurupa G, Tsonev L, Medved L. Structural organization of the fibrin(ogen) αC-domain. Biochemistry 2002;41:6449–6459. [PubMed: 12009908]

8. Burton RA, Tsurupa G, Medved L, Tjandra N. Identification of an ordered compact structure within the recombinant bovine fibrinogen αC-domain fragment by NMR. Biochemistry 2006;45:2257–2266. [PubMed: 16475814]
9. Lewis SD, Shields PP, Shafer JA. Characterization of the kinetic pathway for liberation of fibrinopeptides during assembly of fibrin. J Biol Chem 1985;260:10192–10199. [PubMed: 4019507]
10. Ruf W, Bender A, Lane DA, Preissner KT, Selmayr E, Muller-Berghaus G. Thrombin-induced fibrinopeptide B release from normal and variant fibrinogens: influence of inhibitors of fibrin polymerization. Biochim Biophys Acta 965:169–175. [PubMed: 3365451]
11. Weisel JW. Fibrin assembly. Lateral aggregation and the role of the two pairs of fibrinopeptides. Biophys J 1986;50:1079–1093. [PubMed: 3801570]
12. Weisel JW, Veklich Y, Gorkun O. The sequence of cleavage of fibrinopeptides from fibrinogen is important for protofibril formation and enhancement of lateral aggregation in fibrin clots. J Mol Biol 1993;232:285–297. [PubMed: 8331664]
13. Doolittle RF. Fibrinogen and fibrin. Annu Rev Biochem 1984;53:195–229. [PubMed: 6383194]
14. Ariens RA, Lai TS, Weisel JW, Greenberg CS, Grant PJ. Role of factor XIII in fibrin clot formation and effects of genetic polymorphisms. Blood 2002;100:743–754. [PubMed: 12130481]
15. Mosesson MW, Alkjaersig N, Sweet B, Sherry S. Human fibrinogen of relatively high solubility. Comparative biophysical, biochemical, and biological studies with fibrinogen of lower solubility. Biochemistry 1967;6:3279–3287. [PubMed: 6056988]
16. Holm B, Brosstad F, Kierulf P, Godal HC. Polymerization properties of two normally circulating fibrinogens, HMW and LMW. Evidence that the COOH-terminal end of the α-chain is of importance for fibrin polymerization. Thromb Res 1985;39:595–606. [PubMed: 4082102]
17. Medved LV, Gorkun OV, Manyakov VF, Belitser VA. The role of fibrinogen αC-domains in the fibrin assembly process. FEBS Lett 1985;181:109–112. [PubMed: 3972099]
18. Weisel JW, Papsun DM. Involvement of the COOH-terminal portion of the α-chain of fibrin in the branching of fibers to form a clot. Thromb Res 1987;47:155–163. [PubMed: 2958957]
19. Gorkun OV, Veklich YI, Medved LV, Henschen AH, Weisel JW. Role of the αC domains of fibrin in clot formation. Biochemistry 1994;33:6986–6997. [PubMed: 8204632]
20. Koopman J, Haverkate F, Grimbergen J, Egbring R, Lord ST. Fibrinogen Marburg: a homozygous case of dysfibrinogenemia, lacking amino acids Aα 461–610 (Lys 461 AAA-->stop TAA). Blood 1992;80:1972–1979. [PubMed: 1391954]
21. Koopman J, Haverkate F, Grimbergen J, Lord ST, Mosesson MW, DiOrio JP, Siebenlist KS, Legrand C, Soria J, Soria C, et al. Molecular basis for fibrinogen Dusart (Aα 554 Arg-->Cys) and its association with abnormal fibrin polymerization and thrombophilia. J Clin Invest 1993;91:1637–1643. [PubMed: 8473507]
22. Siebenlist KR, Mosesson MW, DiOrio JP, Soria J, Soria C, Caen JP. The polymerization of fibrinogen Dusart (Aα 554 Arg-->Cys) after removal of carboxy terminal regions of the Aα-chains. Blood Coagul Fibrinolysis 1993;4:61–65. [PubMed: 8457653]
23. Wada Y, Lord ST. A correlation between thrombotic disease and a specific fibrinogen abnormality (Aα 554 Arg-->Cys) in two unrelated kindred, Dusart and Chapel Hill III. Blood 1994;84:3709–3714. [PubMed: 7949126]
24. Furlan M, Steinmann C, Jungo M, Bogli C, Baudo F, Redaelli R, Fedeli F, Lammle B. A frameshift mutation in Exon V of the Aα-chain gene leading to truncated Aα-chains in the homozygous dysfibrinogen Milano III. J Biol Chem 1994;269:33129–33134. [PubMed: 7806542]
25. Baradet TC, Haselgrove JC, Weisel JW. Three-dimensional reconstruction of fibrin clot networks from stereoscopic intermediate voltage electron microscope images and analysis of branching. Biophys J 1995;68:1551–1560. [PubMed: 7787040]
26. Collet JP, Woodhead JL, Soria J, Soria C, Mirshahi M, Caen JP, Weisel JW. Fibrinogen Dusart: electron microscopy of molecules, fibers and clots, and viscoelastic properties of clots. Biophys J 1996;70:500–510. [PubMed: 8770228]
27. Woodhead JL, Nagaswami C, Matsuda M, Arocha-Pinango CL, Weisel JW. The ultrastructure of fibrinogen Caracas II molecules, fibers, and clots. J Biol Chem 1996;271:4946–4953. [PubMed: 8617768]

28. Ridgway HJ, Brennan SO, Gibbons S, George PM. Fibrinogen Lincoln: a new truncated α chain variant with delayed clotting. Br J Haematol 1996;93:177–184. [PubMed: 8611457]
29. Ridgway HJ, Brennan SO, Faed JM, George PM. Fibrinogen Otago: a major α chain truncation associated with severe hypofibrinogenaemia and recurrent miscarriage. Br J Haematol 1997;98:632–639. [PubMed: 9332319]
30. Gorkun OV, Henschen-Edman AH, Ping LF, Lord ST. Analysis of Aα251 fibrinogen: the αC domain has a role in polymerization, albeit more subtle than anticipated from the analogous proteolytic fragment X. Biochemistry 1998;37:15434–15441. [PubMed: 9799505]
31. Vlietman JJ, Verhage J, Vos HL, van Wijk R, Remijn JA, van Solinge WW, Brus F. Congenital afibrinogenaemia in a newborn infant due to a novel mutation in the fibrinogen Aα gene. Br J Haematol 2002;119:282–283. [PubMed: 12358944]
32. Collet JP, Moen JL, Veklich YI, Gorkun OV, Lord ST, Montalescot G, Weisel JW. The αC domains of fibrinogen affect the structure of the fibrin clot, its physical properties, and its susceptibility to fibrinolysis. Blood 2005;106:3824–3830. [PubMed: 16091450]
33. Veklich YI, Gorkun OV, Medved LV, Nieuwenhuizen W, Weisel JW. Carboxyl-terminal portions of the α chains of fibrinogen and fibrin. Localization by electron microscopy and the effects of isolated αC fragments on polymerization. J Biol Chem 1993;268:13577–13585. [PubMed: 8514790]
34. Lau HK. Anticoagulant function of a 24-Kd fragment isolated from human fibrinogen A α chains. Blood 1993;81:3277–3284. [PubMed: 8507865]
35. Cierniewski CS, Plow EF, Edgington TS. Conformation of the carboxy-terminal region of the Aα chain of fibrinogen as elucidated by immunochemical analyses. Eur J Biochem 1984;141:489–496. [PubMed: 6204869]
36. Cierniewski CS, Budzynski AZ. Involvement of the alpha chain in fibrin clot formation. Effect of monoclonal antibodies. Biochemistry 1992;31:4248–4253. [PubMed: 1373653]
37. Sobel JH, Gawinowicz MA. Identification of the α chain lysine donor sites involved in factor XIIIa fibrin cross-linking. J Biol Chem 1996;271:19288–19297. [PubMed: 8702612]
38. Matsuka YV, Medved LV, Migliorini MM, Ingham KC. Factor XIIIa-catalyzed cross-linking of recombinant αC fragments of human fibrinogen. Biochemistry 1996;35:5810–5816. [PubMed: 8639541]
39. Tsurupa G, Veklich Y, Hantgan R, Belkin AM, Weisel JW, Medved L. Do the isolated fibrinogen αC-domains form ordered oligomers? Biophys Chem 2004;112:257–266. [PubMed: 15572257]
40. Belkin AM, Tsurupa G, Zemskov E, Veklich Y, Weisel JW, Medved L. Transglutaminase-mediated oligomerization of the fibrin(ogen) αC domains promotes integrin-dependent cell adhesion and signaling. Blood 2005;105:3561–3568. [PubMed: 15637140]
41. Gorkun OV, Litvinov RI, Veklich YI, Weisel JW. Interactions mediated by the N-terminus of fibrinogen's Bβ chain. Biochemistry 2006;45:14843–14852. [PubMed: 17144678]
42. Doolittle RF, Kollman JM. Natively unfolded regions of the vertebrate fibrinogen molecule. Proteins 2006;63:391–397. [PubMed: 16288455]
43. Ashkin A. Optical trapping and manipulation of neutral particles using lasers. Proc. Natl Acad. Sci. USA 1997;94:4852–4860.
44. Litvinov RI, Shuman H, Bennett JS, Weisel JW. Binding strength and activation state of single fibrinogen-integrin pairs on living cells. Proc Natl Acad Sci USA 2002;99:7426–7431. [PubMed: 12032299]
45. Litvinov RI, Bennett JS, Weisel JW, Shuman H. Multi-step fibrinogen binding to the integrin αIIbβ3 detected using force spectroscopy. Biophys J 2005;89:2824–2834. [PubMed: 16040750]
46. Litvinov RI, Gorkun OV, Owen SF, Shuman H, Weisel JW. Polymerization of fibrin: specificity, strength, and stability of knob-hole interactions studied at the single-molecule level. Blood 2005;106:2944–2951. [PubMed: 15998829]
47. Litvinov RI, Gorkun OV, Galanakis DK, Yakovlev S, Medved L, Shuman H, Weisel JW. Polymerization of fibrin: Direct observation and quantification of individual B:b knob-hole interactions. Blood 2007;109:130–138. [PubMed: 16940416]
48. Tsurupa G, Medved L. Identification and characterization of novel tPA- and plasminogen-binding sites within fibrin(ogen) αC-domains. Biochemistry 2001;40:801–808. [PubMed: 11170397]

49. Gorlatov S, Medved L. Interaction of fibrin(ogen) with the endothelial cell receptor VE-cadherin: mapping of the receptor-binding site in the NH_2-terminal portions of the fibrin β chains. Biochemistry 2002;41:4107–4116. [PubMed: 11900554]
50. Kudryk B, Rohoza A, Ahadi M, Chin J, Wiebe ME. A monoclonal antibody with ability to distinguish between NH_2-terminal fragments derived from fibrinogen and fibrin. Mol Immunol 1983;20:1191–1200. [PubMed: 6656769]
51. Procyk R, Kudryk B, Callender S, Blomback B. Accessibility of epitopes on fibrin clots and fibrinogen gels. Blood 1991;77:1469–1475. [PubMed: 1706954]
52. Blomback B, Hessel B, Iwanaga S, Reuterby J, Blomback M. Primary structure of human fibrinogen and fibrin. I. Clevage of fibrinogen with cyanogen bromide. Isolation and characterization of NH_2-terminal fragments of the ("A") chain. J Biol Chem 1972;247:1496–1512. [PubMed: 5012319]
53. Blomback B, Hessel B, Hogg D. Disulfide bridges in NH_2-terminal part of human fibrinogen. Thromb Res 1976;8:639–658. [PubMed: 936108]
54. Ashkin A. Forces of a single-beam gradient laser trap on a dielectric sphere in the ray optics regime. Biophys. J 1992;61:569–582.
55. Svoboda K, Block SM. Biological applications of optical forces. Annu. Rev. Biomol. Struct 1994;23:247–285.
56. Smith SB, Cui Y, Bustamante C. Overstretching B-DNA: the elastic response of individual double-stranded and single-stranded DNA molecules. Science 1996;271:795–799. [PubMed: 8628994]
57. Allersma MW, Gittes F, deCastro MJ, Stewart RJ, Schmidt CF. Two-dimensional tracking of ncd motility by back focal plane interferometry. Biophys J 1998;74:1074–1085. [PubMed: 9533719]
58. Visscher K, Gross SP, Block SM. Construction of multiple-beam optical traps with nanometer-resolution position sensing. IEEE J. Select. Topics Quant. Electronics 1996;2:1066–1076.
59. Privalov PL, Medved LV. Domains in the fibrinogen molecule. J Mol Biol 1982;159:665–683. [PubMed: 7143446]
60. Medved LV, Gorkun OV, Privalov PL. Structural organization of C-terminal parts of fibrinogen Aα-chains. FEBS Lett 1983;160:291–295. [PubMed: 6224704]
61. Erickson HP, Fowler WE. Electron microscopy of fibrinogen, its plasmic fragments and small polymers. Ann N Y Acad Sci 1983;408:146–163. [PubMed: 6575682]
62. Mosesson MW, Hainfeld J, Wall J, Haschemeyer RH. Identification and mass analysis of human fibrinogen molecules and their domains by scanning transmission electron microscopy. J Mol Biol 1981;153:695–718. [PubMed: 7338923]
63. Weisel JW, Stauffacher CV, Bullitt E, Cohen C. A model for fibrinogen: domains and sequence. Science 1985;230:1388–1391. [PubMed: 4071058]
64. Leckband DE, Schmitt FJ, Israelachvili JN, Knoll W. Direct force measurements of specific and nonspecific protein interactions. Biochemistry 1994;33:4611–4624. [PubMed: 8161517]
65. Zhu C, Long M, Chesla SE, Bongrand P. Measuring receptor/ligand interaction at the single-bond level: experimental and interpretative issues. Ann Biomed Eng 2002;30:305–314. [PubMed: 12051616]

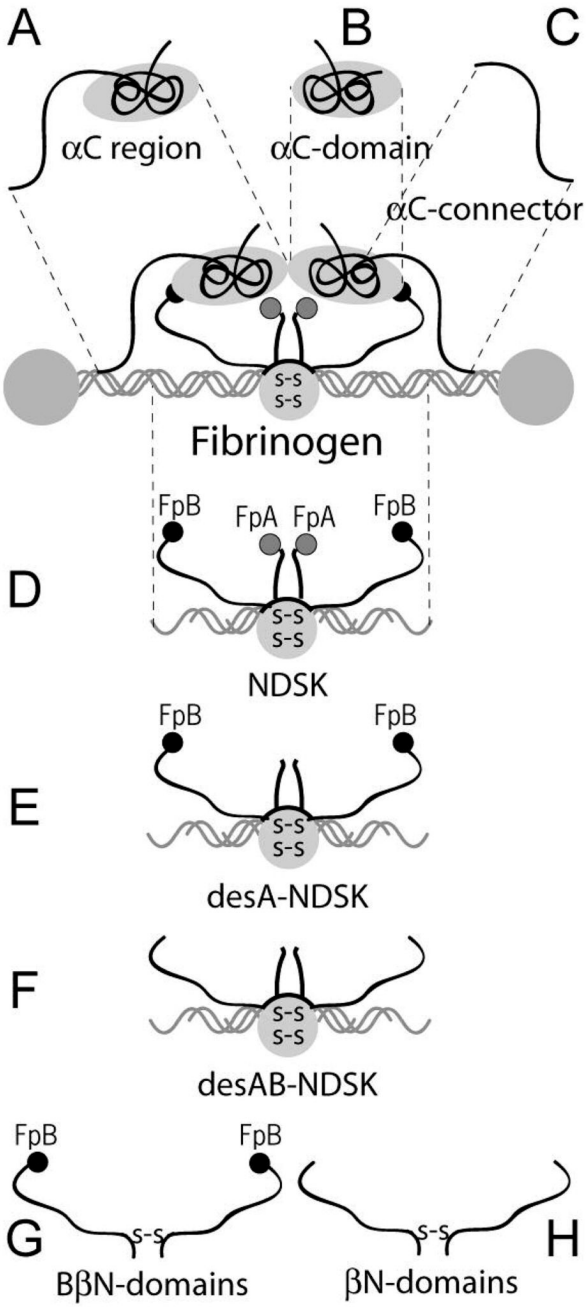

Figure 1. Cartoon of fibrinogen and fibrin(ogen) fragments used in this study

A, B, and **C** show the αC region fragment corresponding to the C-terminal portion of the fibrinogen Aα chain (residues Aα221-610) and its sub-fragments, the αC-domain (residues Aα392-610) and αC-connector (residues Aα221-391), respectively. **D**, **E**, and **F** show NDSK ["N-Terminal DiSulphide Knot"(3)], a fragment from the central part of fibrinogen containing both FpA and FpB, desA-NDSK with cleaved FpA but remaining FpB, and desAB-NDSK with both FpA and FpB cleaved, respectively. **G** shows the recombinant fibrinogen $(B\beta 1\text{-}66)_2$ fragment consisting of two BβN-domains formed by the N-terminal portions of the fibrinogen Bβ chain. **H** shows the recombinant fibrin fragment $(\beta 15\text{-}66)_2$ including two βN-domains devoid of fibrinopeptides B. The grey and black circles on the ends represent

fibrinopeptides A (FpA) and B (FpB), respectively. The gray circle in the center with double designations “S-S” inside represents a cluster of disulphide bonds.

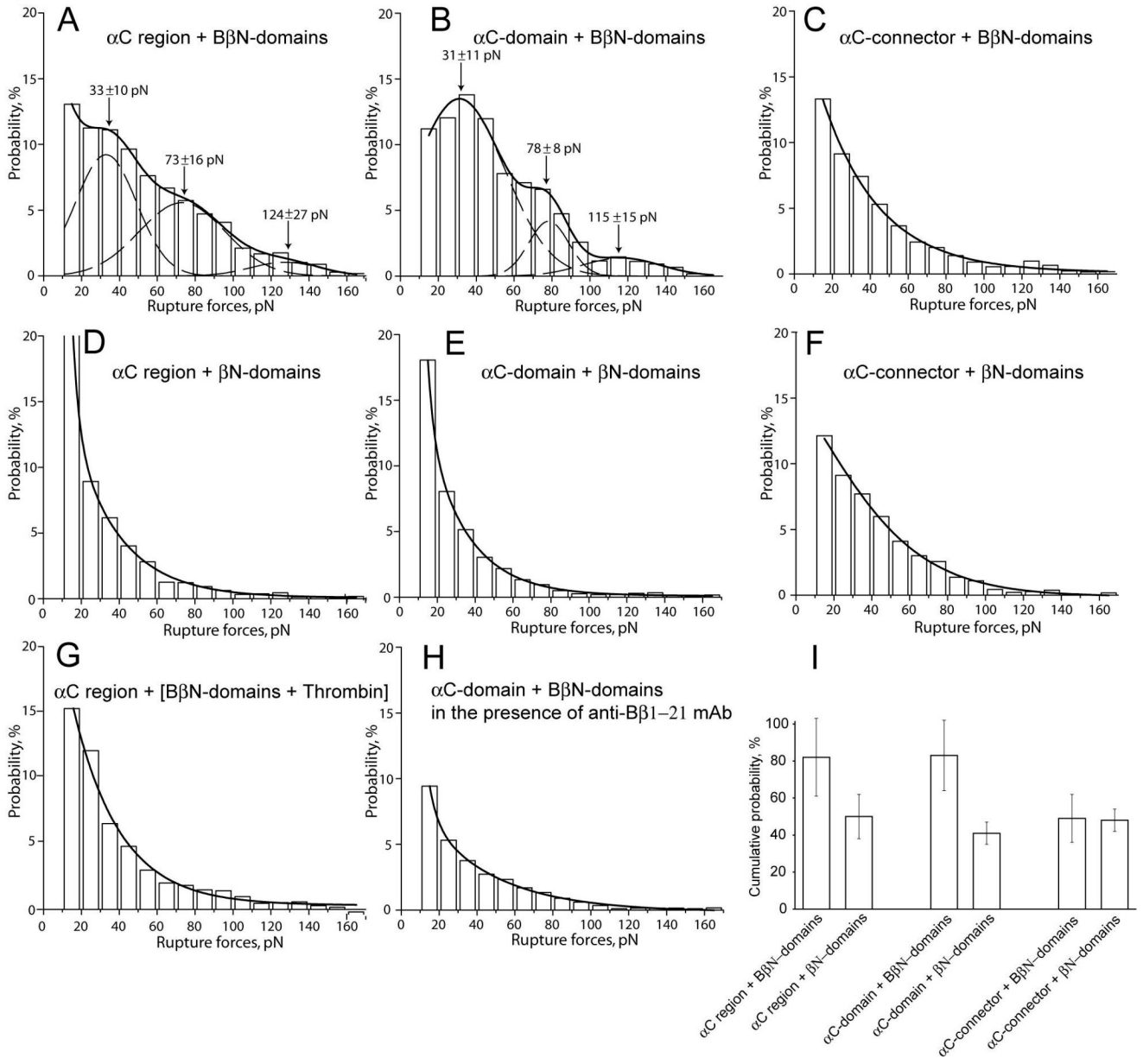

Figure 2. The panel of rupture force histograms demonstrating interactions of the recombinant fragment corresponding to the αC region and its sub-fragments, αC-connector and αC-domain, with the recombinant $(Bβ1\text{-}66)_2$ and $(β15\text{-}66)_2$ fragments corresponding to the fibrinogen BβN- and fibrin βN-domains, respectively

A, B, and **C** – interactions of the BβN-domains with the αC region, αC-domain, and αC-connector, respectively; **D, E,** and **F** - interactions of the βN-domains with the αC region, αC-domain, and αC-connector, respectively; **G** - interactions of the αC region with the BβN-domains treated with thrombin and thus converted to the βN-domains right on the surface; **H** - interactions of the αC-domain with the BβN-domains in the presence of 200 μg/ml anti-Bβ1-21 mAb; **I** – paired bars representing cumulative probabilities of forces >10 pN derived from A and D, B and E, and C and F. The dashed lines show the fitting with Gaussian curves to determine the position of each peak that corresponds to the most probable rupture force.

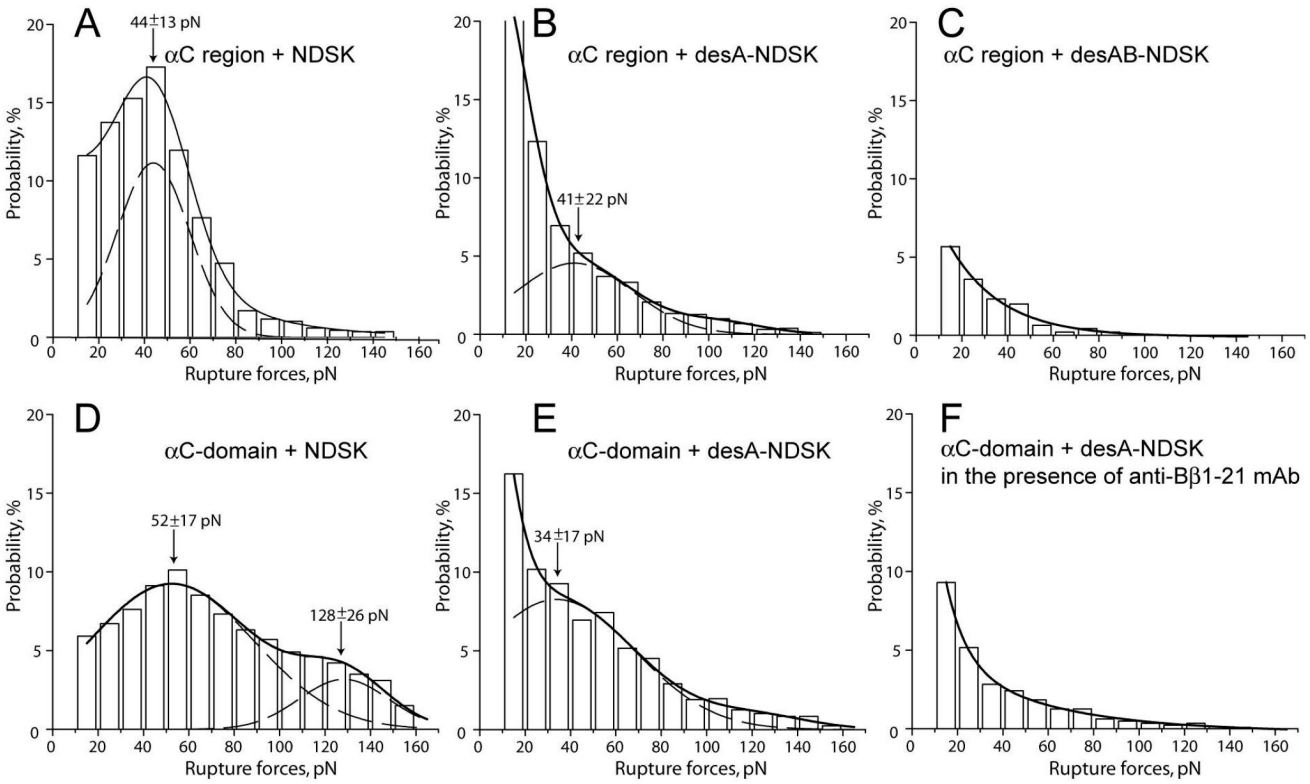

Figure 3. The panel of rupture force histograms demonstrating interactions of the recombinant αC region and αC-domain with various NDSK fragments corresponding to the central E region of fibrin(ogen)

A, B, and **C** - interactions of the αC region with NDSK, desA-NDSK, and desAB-NDSK, respectively; **D** and **E** - interactions of the αC-domain with NDSK and desA-NDSK, respectively; **F** – the same as in E, but in the presence of 200 μg/ml anti-Bβ1-21 mAb. The dashed lines show the fitting with Gaussian curves to determine the position of each peak that corresponds to the most probable rupture force.

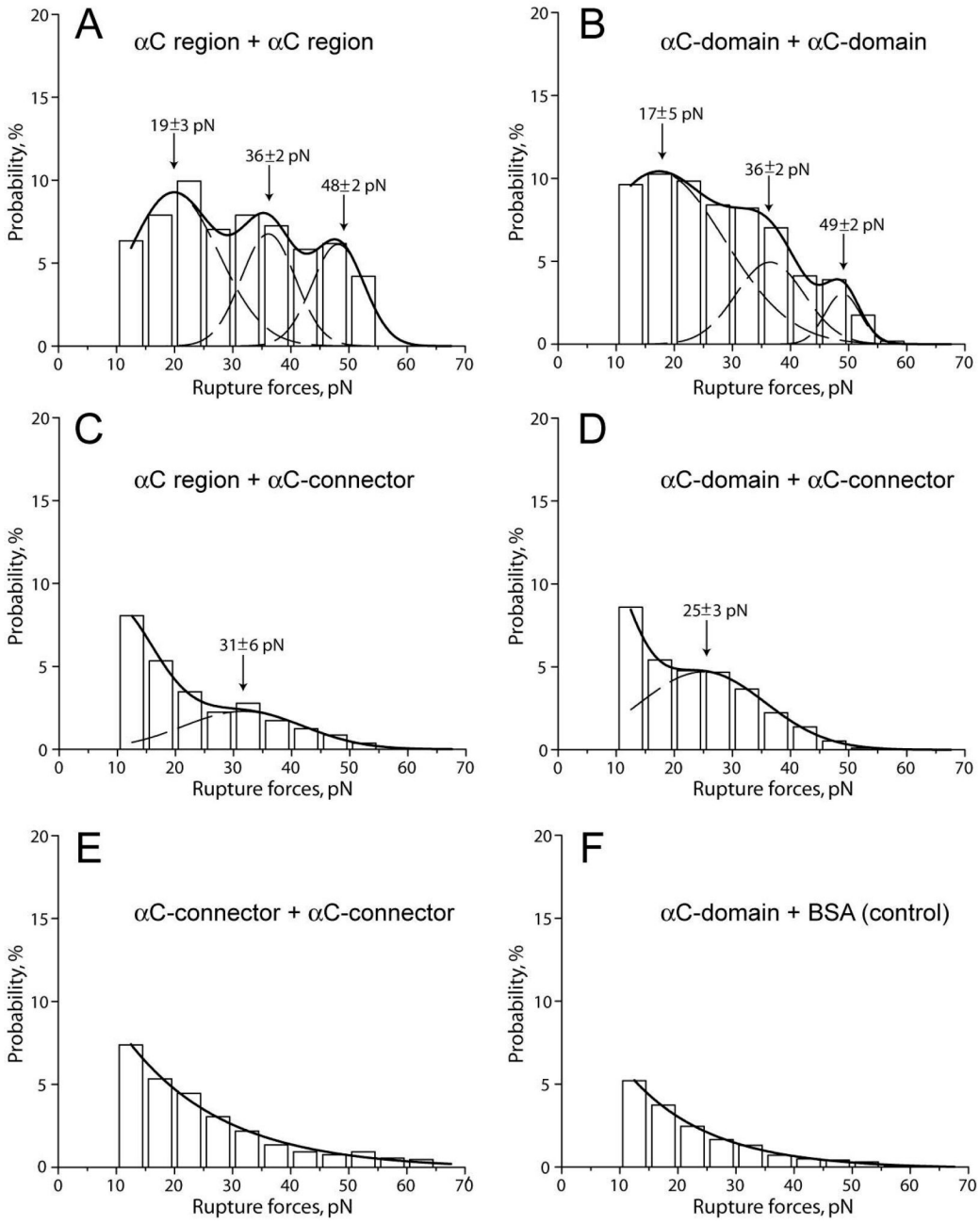

Figure 4. The panel of rupture force histograms demonstrating interactions of the αC region and its sub-fragments, αC-domain and αC-connector

A - interactions of the pedestal-bound αC region with the αC region coupled to a bead; **B** - the pedestal-bound αC-domain with the αC-domain coupled to a bead; **C, D,** and **E** – the pedestal-bound αC region, αC-domain, and αC-connector with the αC-connector coupled to a bead, respectively; **F** - the pedestal-bound αC-domain with the BSA-coated bead (negative control). The dashed lines show the fitting with Gaussian curves to determine the position of each peak that corresponds to the most probable rupture force.

Table 1

Cumulative binding probability (all rupture forces >10 pN) for different interacting proteins

Interacting proteins	Cumulative probability, %	The most probable rupture force, pN			Corresponding figure and graph #
		Peak 1	Peak 2	Peak 3	
αC region + BβN-domains	82±21	33±10	73±16	124±27	2A
αC-domain + BβN-domains	83±19	31±11	78±8	115±15	2B
αC-connector + BβN-domains	49±13	No peak	No peak	No peak	2C
αC region + βN-domain	50±12	No peak	No peak	No peak	2D
αC-domain + βN-domains	41±6	No peak	No peak	No peak	2E
αC-connector + βN-domains	48±6	No peak	No peak	No peak	2F
αC-domain + [BβN-domains + thrombin]	52±11	No peak	No peak	No peak	2G
αC-domain + [BβN-domains + anti-Bβ1-21 mAb]	29±6	No peak	No peak	No peak	2H
αC-domain + BβN-domains at 1/10 surface density	35±5	No peak	No peak	No peak	Not shown
αC-domain at 1/10 surface density + BβN-domains	26±7	No peak	No peak	No peak	Not shown
αC region + NDSK	88±17	44±13	No peak	No peak	3A
αC region + desA-NDSK	59±9	41±22	No peak	No peak	3B
αC region + desAB-NDSK	15±4	No peak	No peak	No peak	3C
αC-domain + NDSK	89±22	52±17	No peak	No peak	3D
αC-domain + [NDSK + anti-Bβ1-21 mAb]	56±12	No peak	No peak	No peak	Not shown
αC-domain + desA-NDSK	71±14	34±17	No peak	No peak	3E
αC-domain + [desA-NDSK + anti-Bβ1-21 mAb]	26±11	No peak	No peak	No peak	3F
αC-domain + desAB-NDSK	18±5	No peak	No peak	No peak	Not shown
αC region + αC region	62±10	19±3	36±2	48±2	4A
αC region + αC-domain	63±12	17±5	36±2	49±2	4B
αC region + αC-connector	26±6	31±6	No peak	No peak	4C
αC-domain + αC-connector	31±7	25±3	No peak	No peak	4D
αC-connector + αC-connector	27±5	No peak	No peak	No peak	4E
αC-domain + BSA (negative control)	16±4	No peak	No peak	No peak	4F
αC region + BSA (negative control)	21±6	No peak	No peak	No peak	Not shown

Note: Values are expressed as mean ± SD